MAX-PLANCK-INSTITUT FÜR PLASMAPHYSIK

GARCHING BEI MÜNCHEN

2-D Fluid Calculations of Anomalous Trapped Ion Transport in Tokamaks

R. Saison, H.K. Wimmel, and F. Sardei

IPP 6/156 March 1977

Die nachstehende Arbeit wurde im Rahmen des Vertrages zwischen dem Max-Planck-Institut für Plasmaphysik und der Europäischen Atomgemeinschaft über die Zusammenarbeit auf dem Gebiete der Plasmaphysik durchgeführt.

IPP 6/156

R. Saison, H.K. Wimmel
and F. Sardei

2-D Fluid Calculations of Anomalous Trapped Ion Transport in Tokamaks

March 1977 (in English)

Abstract

The collisional, nonlinear trapped-fluid equations of Kadomtsev and Pogutse (K.P.) are used as a description of the dissipative trapped-ion modes. The equations are solved numerically in two spatial dimension as an initial-value problem, with due observation of the appropriate boundary conditions, which are derived. Numerical results are given for the resulting anomalous diffusion coefficient D at late times, when the dissipative trapped-ion instability saturates. In terms of appropriate units, D is found to depend, in essence, on one dimensionless parameter only. Examples of the time development D(t) are also given. The numerical values of D (at late times) are generally <u>larger</u> than according to the K.P. formula, and the scaling of D with the equilibrium parameters resembles <u>Bohm scaling.</u> The dependence of the results on the numerical grid and on the initial conditions was also studied. In addition, several analytical results are presented, some of which have been successfully used for testing the numerical code.

1. Introduction

An estimate given by KADOMTSEV and POGUTSE (1967, 1970, 1971) shows it to be probable that in future large tokamaks the anomalous particle and energy transports in the plasma will depend critically on the dissipative trapped-ion instability (DTII) (see list of references). It is not clear whether the K.P. estimate, on the one hand, and 1-D numerical calculations by the Princeton group (COHEN et al., 1976), on the other hand, are reliable (see Sec. 10). It is therefore important to check those results by more elaborate calculations. We present here the first successful 2-D numerical calculations of the saturation of the dissipative trapped-ion mode, together with the resulting anomalous diffusion coefficients.

Generally, two different approaches can be adopted in order to obtain a quantitative description of the DTII. On the one hand, one merely calculates the linearly unstable parameter ranges and the linear growth rates and frequencies of the various modes, without investigating the magnitude of the anomalous transport. This linear analysis has been done by several authors using kinetic equations, considering complex equilibrium situations and including various particle effects. See, for instance, COPPI et al. (1976), GLADD et al. (1973), ROSENBLUTH et al. (1972), TANG (1973, 1974), TANG et al. (1976). On the other hand, one aims at calculating the time-asymptotic plasma state in order to determine the saturation level of the modes and the anomalous diffusion of plasma particles. See WIMMEL (1976/1 and 1976/2) and COHEN (1976). This nonlinear problem calls for greater simplification of the physical assumptions; that is, a fluid-type theory is to be preferred, at least for the time being. This is the line followed in this paper.

We shall therefore use the 2-D, collisional transport equations that describe the particle balance for the ions and electrons trapped in the toroidal $\underset{\sim}{B}$ - field, as formulated by KADOMTSEV and POGUTSE (1970, 1971). See Secs. 2 and 3. These equations will be solved numerically (see Secs. 8 and 9). Here, it should be borne in mind that the K.P. equations also admit of discontinuous solutions (Sec. 5), which, however, are thought to be physically unrealistic. Effects omitted in the K.P. equations (e.g. finite gyroradii, neoclassical diffusion, viscosity, Landau damping) lead one to expect smooth field distributions in real plasmas. It is therefore a matter of finding a numerical code which does not produce any undesirable singularities, and one must verify that the anomalous diffusion calculated depends only insignificantly on the discretization chosen. Otherwise additional smoothing terms must be added in the equations. Other effects that are neglected by the K.P. equations include the correct influence of the electric field component parallel to $\underset{\sim}{B}$ on the trapped and free particles and the effect of $\nabla \delta_0$, where δ_0 is the equilibrium fraction of trapped particles (see WIMMEL, 1975 and 1976/1). Both corrections will be ignored here for the sake of simplicity.

In addition, several analytic properties of the K.P. equations will be discussed. These properties can be used to check the numerical computations.

The paper is organized as follows: The K.P. equations are introduced in Secs. 2 and 3. In Sec. 4 the necessary boundary conditions are established. Bounds for the solutions and invariance properties are listed in Sec. 5. Section 6 presents necessary conditions for travelling wave solutions, while a dimensional analysis of the parameter dependence of the anomalous diffusion coefficient is given in Sec. 7. In Sec. 8 the method of computation is briefly described, and numerical results are given in Sec. 9. In Sec. 10 the meaning and the reliability of the results are discussed and 1-D and 2-D calculations are compared. Section 11 gives a summary.

2. General Equations

The Kadomtsev-Pogutse equations are (KADOMTSEV and POGUTSE, 1967, 1970, 1971; WIMMEL, 1976/1)

$$n^i_t + \nu_i \left(n^i - n^0\right) + \nabla\cdot\left(n^i \underset{\sim}{v}\right) = 0, \tag{2.1}$$

$$n^e_t + \nu_e \left(n^e - n^0\right) + \nabla\cdot\left(n^e \underset{\sim}{v}\right) = 0, \tag{2.2}$$

$$\phi = \frac{T}{2eN^0}\left(n^i - n^e\right), \tag{2.3}$$

$$\underset{\sim}{v} = -\frac{c}{B}\hat{z}\times\nabla\phi = \hat{z}\times\nabla\left[A\left(n^i - n^e\right)\right], \tag{2.4}$$

$$\nabla \underset{\sim}{B} = 0 \quad , \quad \nabla\cdot\underset{\sim}{v} = 0, \tag{2.5/6}$$

$$A = \frac{cT}{2eBN^0} \quad , \quad T = \frac{2T_e T_i}{T_e + T_i}. \tag{2.7/8}$$

These equations describe the 2-D, $\underset{\sim}{E}\times\underset{\sim}{B}$ drift motion of the trapped ions and electrons in a plasma slab and their interaction (creation, annihilation) with the background of untrapped particles by collisional equations of continuity for the trapped particles. The electric potential is obtained from the quasineutrality condition for both trapped and untrapped particles. The coordinates used are x, y, and the time t. Given quantities are the magnetic field $\underset{\sim}{B}$, the temperatures $T_{i,e}(x)$ and the density $N^P(x)$ in equilibrium. The equilibrium densities of trapped and untrapped particles, respectively, are $n^0(x) = \delta_0(x) \cdot N^p(x)$ and $N^0(x)$ $= [1-\delta_0(x)] \cdot N^p(x)$. The effective collision frequencies for trapped particles are $\nu_{i,e} \approx \nu_{i,e}^{COUL} / \delta_0^2$. The unknown functions $n^{i,e}(x,y,t) \geqq 0$ are the trapped particle densities, ϕ is the electric potential, and $\underset{\sim}{v}$ is the $\underset{\sim}{E} \times \underset{\sim}{B}$ drift velocity. The subscript t designates the time-derivative. Equations (2.1) to (2.4) are to be solved using appropriate initial and boundary conditions (see Sec. 4). The plasma slab extends over $0 \leqq x \leqq a$, with walls at $x = 0$ and $x = a$. The plasma is periodic in the y direction, with the periodicity length b (b of the order of a).

For general $A(x), \nabla A \not\equiv 0$, the K.P. equations have the following <u>special solutions,</u> which are damped and have vanishing particle flux density in the x - direction:

$$n^i = n^0(x) + n_1^i(x) \exp(-\nu_i t), \tag{2.9}$$

$$n^e = n^0(x) + n_1^e(x) \exp(-\nu_e t), \tag{2.10}$$

where n_1^i and n_1^e can be chosen arbitrarily as long as $n^{i,e} \geqq 0$ and the boundary conditions (see Sec. 4 below) are satisfied. These solutions make the nonlinear terms of the K.P. equations vanish separately. In particular, n_1^i and n_1^e can be chosen as sums of Heaviside step functions, wich shows that the K.P. equations allow discontinuous solutions.

In Sec. 4 we shall see that the appropriate boundary conditions to the K.P. equations forbid trapped particle flux densities to the walls. Hence, simple equations of motion can be derived for the total trapped-particle numbers,

$$Z^{i,e}(t) =: \int_0^a dx \int_0^b dy \; n^{i,e}(x, y, t), \tag{2.11}$$

viz. if $\nabla \nu_{i,e} = 0$:

$$Z_t^i + \nu_i (Z^i - Z^o) = 0, \tag{2.12}$$

with the general solutions:

$$Z^i = Z^o + (Z^{io} - Z^o) \exp(-\nu_i t). \tag{2.13}$$

Here Z^{io} is the initial value of Z^i, and

$$Z^o =: \int_0^a dx \int_0^b dy \; n^o(x). \tag{2.14}$$

A similar result obtains, of course, for the trapped electrons. It follows that the total trapped charge, i.e. $Q = Z^i - Z^e$, relaxes to zero for $t \to \infty$.

3. Spezialized Equations

It is of advantage to consider the K.P. equations in the approximation $\partial A/\partial x = 0$. This condition can, on the one hand, be interpreted as a special equilibrium with $T/N^{o} =$ const. Of course, the assumption $\nu_{i,e}$ = const, i.e. $N^{p}/T^{3/2}\,\delta_0^2 =$ const, then generally assumes the character of an approximation. On the other hand, the condition can be interpreted as a restriction of equilibria and perturbations such that almost everywhere

$$|\partial_x \ln (T/N^{o})| \ll |\partial_x \ln \varrho| , \tag{3.1}$$

with $\varrho = n^{i} - n^{e}$ being the trapped charge density divided by e. If $\partial_x A = 0$, then the drift velocity $\underset{\sim}{v}$ is tangential to the instantaneous $\varrho =$ const contours, viz. $\underset{\sim}{v} = A\hat{z} \times \nabla\varrho$ and $\underset{\sim}{v} \cdot \nabla\varrho = 0$, and the following form of the K.P. equations obtains:

$$n^{i}_{t} + \nu_i (n^{i} - n^{o}) + A(n^{i}_{x} n^{e}_{y} - n^{i}_{y} n^{e}_{x}) = 0, \tag{3.2}$$

$$n^{e}_{t} + \nu_e (n^{e} - n^{o}) + A(n^{i}_{x} n^{e}_{y} - n^{i}_{y} n^{e}_{x}) = 0, \tag{3.3}$$

where the subcripts x and y denote spatial derivatives. Consequently, the following linear relation holds:

$$\varrho_t + \nu_i (n^{i} - n^{o}) - \nu_e (n^{e} - n^{o}) = 0. \tag{3.4}$$

The system of eqs. (3.2), (3.3) may also be transformed into the following second-order equation, if $\nabla \nu_{i,e} = 0$, viz.

$$\rho_{tt} + (\nu_i + \nu_e)\,\rho_t + \nu_i \nu_e\, \rho - (\nu_e - \nu_i)\, v_0\, \rho_y$$

$$+ A(\rho_x \rho_{yt} - \rho_y \rho_{xt}) = 0, \tag{3.5}$$

with the diamagnetic drift velocity $v_0 = A n^0_x$. Often $\nabla v_0 = 0$ is assumed, but, in general, v_0 may depend on x. The trapped densities $n^{i,e}$ can be obtained from ρ and ρ_t :

$$n^i = n^0 + (\nu_e - \nu_i)^{-1} (\rho_t + \nu_e \rho), \tag{3.6}$$

$$n^e = n^0 + (\nu_e - \nu_i)^{-1} (\rho_t + \nu_i \rho). \tag{3.7}$$

From eqs. (3.5) to (3.7) and periodicity in y it is readily derived that the specialized K.P. equations permit only one time-independent solution, namely the equilibrium $\rho = 0$, $n^i = n^e = n^0$. In particular, no stationary convection exists in the laboratory system. The linear dispersion equation reads (WIMMEL, 1976/1):

$$(-i\omega + \gamma)^2 + (\nu_e + \nu_i)(-i\omega + \gamma)$$

$$- i(\nu_e - \nu_i)\,\omega_0 + \nu_e \nu_i = 0, \tag{3.8}$$

where ω is the real frequency, γ the growth rate, $\omega_0 = K_y v_0$. The instability condition is

$$\omega_0^2 > \nu_i \nu_e \left(\frac{\nu_e - \nu_i}{\nu_e + \nu_i} \right)^2 . \tag{3.9}$$

Furthermore (WIMMEL, 1976/1), the average particle flux density in the x-direction is ambipolar and may be expressed as

$$\Gamma^x =: \langle n^{i,e} v^x \rangle = -\frac{A}{\nu_e - \nu_i} \langle \rho_t \cdot \rho_y \rangle, \tag{3.10}$$

where the pointed brackets denote the average over y .

A simple differential relation exists between the time-asymptotic particle flux in the x-direction and the electric potential ϕ , both averaged over y and late times t . From eqs. (2.1), (2.2) it follows that

$$\bar{\Gamma}^x{}_x = -\nu_i \langle\langle n^i - n^0 \rangle\rangle = -\nu_e \langle\langle n^e - n^0 \rangle\rangle, \tag{3.11}$$

where the bar denotes the time average and the double pointed brackets indicate averaging over y and t . Owing to eqs. (2.3), (3.6), (3.7) this can be transformed to yield

$$\bar{\Gamma}^x{}_x = -\frac{\nu_e \nu_i}{\nu_e - \nu_i} \langle\langle \rho \rangle\rangle \tag{3.12}$$

or

$$\bar{\Gamma}^x{}_x = -\frac{2eN^0}{T} \frac{\nu_e \nu_i}{\nu_e - \nu_i} \langle\langle \phi \rangle\rangle . \tag{3.13}$$

It follows that the average potential is negative in the interior and positive near the outer wall $(x = a)$, if $\bar{\Gamma}^x > 0$ in the volume and $\bar{\Gamma}^x = 0$ at the boundaries, as prescribed by the boundary conditions (Sec.4). Another relation, between the particle flux and the mean density $n = \frac{1}{2}(n^i + n^e)$, can also be derived, viz.

$$\bar{\Gamma}^{x}_{\ x} = - \frac{2 \nu_e \nu_i}{\nu_e + \nu_i} \langle\langle n - n^0 \rangle\rangle . \tag{3.14}$$

This formula and eq. (3.11) describe the underpopulation or over-population of the trapped particles (preferably the ions) caused by the divergence of the trapped particle flux (see WIMMEL, 1976/2).

4. Boundary Conditions

Previous authors either did not introduce boundary conditions at all or else only for y because the equations were only intended for estimates or because crude approximations were made. Boundary conditions are indispensable, however, for numerical or analytical calculations of solutions of the K.P. equations.

The slab coordinates x and y represent the coordinates r and $r(\theta - q\zeta)$ in the plasma torus (see LAQUEY et al., 1975) because the surface considered has to be aligned perpendicular to $\underset{\sim}{B}$. Here r is the distance from the magnetic axis, θ and ζ are the poloidal and toroidal angles, and q(r) is the "safety factor". A surface in the torus (or cylinder) everywhere perpendicular to $\underset{\sim}{B}$, with $q \neq \infty$, is a surface that spirals around the magnetic axis. As the dissipative trapped-ion modes considered here are flute-like, it is possible to consider separately a section of the spiral surface which spans an angle $\Delta(\theta - q\zeta) = 2\pi$ and impose periodic boundary conditions in $r(\theta - q\zeta)$ or y. One thus has the intervals $[0, a]$ for r, and $[0, 2\pi r]$ for $r(\theta - q\zeta)$. In the slab model one accordingly chooses the intervals $[0, a]$ for x, and $[0, b]$ for y, with b = a or $b = \pi a$, respectively. It now remains to discuss the boundary conditions for x = 0,a. The minor axis, r = 0, is replaced by a reflecting wall (zero particle fluxes) at x = 0. Because of $n^0_y = 0$ the boundary conditions at x = 0 are then for all times t:

$$v^x = -A\varrho_y = A(n_y^e - n_y^i) = 0 \tag{4.1}$$

and

$$v_t^x = -A\varrho_{yt} = A(\nu_i n_y^i - \nu_e n_y^e) = 0. \tag{4.2}$$

Because of $\nu_i \neq \nu_e$ this yields

$$n_y^i = n_y^e = 0. \tag{4.3}$$

This makes the nonlinear terms of the K.P. equations vanish, which at $x = 0$ thus take the form

$$n_t^{i,e} + \nu_{i,e}(n^{i,e} - n^0) = 0, \tag{4.4}$$

with the general solutions $(x = 0)$:

$$n^{i,e} = n^0 + (n_1^{i,e} - n^0)\exp(-\nu_{i,e} t). \tag{4.5}$$

Here the constants $n_1^{i,e}$ represent the initial densities for $x = t = 0$; they must of course, be independent of y. The K.P. equations can thus be solved at the reflecting wall separately and yield a solution that relaxes towards equilibrium and guarantees $v^x = 0$ for all y and t. In other words, the boundary $x = 0$ with the solutions of eq. (4.5) is a characteristic surface that is isolated from the rest of the volume in the sense that the x-derivatives of $n^{i,e}$ are completely arbitrary at $x = 0$. This leaves v^y undetermined, too; but this does not prevent one solving the K.P. equations at $x = 0$, the reason being that $n_y^i = n_y^e = 0$. The method of characteristics can be used to show that the solution given by eq. (4.5) is unique for given initial data $n_1^{i,e}$, provided $n_1^{i,e}$ are independent of y, and provided the x- derivatives, n_x^i and n_x^e, remain bounded. This means that the above boundary conditions are automatically satisfied in this case once the initial conditions for $t=0$ at the reflecting wall are given. For numerical calculations, however, it is preferable to use the boundary conditions in their explicit form, eq. (4.5), at all times t.

At $x = a$ an <u>absorbing wall</u> is assumed. The boundary conditions there first take the form

$$n^{i,e} \, v^x \geqq 0. \tag{4.6}$$

Because of $n^{i,e} \geqq 0$ this can be rearranged to read

$$\left.\begin{aligned} &v^x \geqq 0 \quad \text{for} \quad n^i + n^e > 0 \\ &v^x \text{ arbitrary for} \quad n^i = n^e = 0 \end{aligned}\right\} \tag{4.7}$$

Owing to the definition of $\underset{\sim}{v}$ as a derivative and the periodicity in y one has for every x and t

$$\int_0^b v^x \, dy = 0. \tag{4.8}$$

If $n^{i,e}$ and v^x are continuous only <u>y-intervals</u> contribute to the integral, either with $n^i + n^e > 0$, or with $n^i = n^e = 0$. Because of $v^x = A(n_y^e - n_y^i)$ the following set of conditions is then equivalent to eq. (4.7) for $x = a$:

$$\left.\begin{array}{lll} v^x \geqq 0 & \text{for} & n^i + n^e > 0 , \\ v^x = 0 & \text{for} & n^i = n^e = 0 . \end{array}\right\} \tag{4.9}$$

Hence, the integral of eq. (4.8) vanishes for $x = a$ only if for all times

$$v^x = 0 , \quad v^x_t = 0 . \tag{4.10}$$

These boundary conditions of the absorbing wall are identical with those of the reflecting wall.

One thus hase the, perhaps, paradoxical result that <u>the K.P. equations do not allow wall losses</u> if $n^{i,e}$, v^x, and, hence ρ_y are continuous. However the collisonal interaction of trapped particles with untrapped ones allows one to have a <u>mean particle flux</u> in the x- direction <u>in the plasma volume</u>, since, for example, trapped particles are created at small values of x and annihilated at large values of x . The anomalous diffusion in the volume can then be calculated in the hope of estimating the wall losses of a real plasma. The above derivation of the boundary conditions holds for the general case with $\nabla A \neq 0$.

5. Bounds and Invariance Properties

Consideration of the K.P. equations in the Lagrangian form

$$\frac{dn^{i,e}}{dt} = -\nu_{i,e}\left(n^{i,e} - n^0\right), \tag{5.1}$$

with

$$\underset{\sim}{v} = \hat{z} \times \nabla\left[A\left(n^i - n^e\right)\right], \tag{5.2}$$

and the definition

$$\frac{dn^j}{dt} = n_t^j + \underset{\sim}{v} \cdot \nabla n^j = n_t^j + \nabla \cdot \left(n^j \underset{\sim}{v}\right), \tag{5.3}$$

for general A(x), i.e. $\nabla A \not\equiv 0$, shows that the property $n^{i,e} \geqq 0$ is preserved in time. Furthermore, one obtains the following upper bounds for $n^{i,e}$ and ρ :

$$n^{i,e} \leqq \max\left(n_1^{i,e}, n^0\right), \tag{5.4}$$

$$|\rho| \leqq \max\left(n_1^i, n_1^e, n^0\right), \tag{5.5}$$

where n_1^i, n_1^e are the initial density profiles. Hence it is seen that <u>the densities remain bounded</u> for all times.

In addition, one can prove that <u>stationary values</u> of n^i , viz. with $\nabla n^i = 0$, or n^e , viz. with $\nabla n^e = 0$, always relax towards equilibrium as long as they do not disappear as such. This may involve stationary points or curves. The <u>proper velocities</u>

$\underset{\sim}{W}^i$ or $\underset{\sim}{W}^e$ of such points or curves must be taken into account. These velocities generally differ from the drift velocity $\underset{\sim}{v}$. Let us consider, for example, a stationary point $\nabla n^i = 0$. Substitution in the K.P. equations, eq. (2.1) to (2.6), yields

$$n^i_t + \nu_i (n^i - n^0) = 0. \qquad (5.6)$$

This equation is also satisfied if the partial time derivative is replaced by the total time derivative taken when moving with the velocity $\underset{\sim}{W}^i$. In fact, both derivatives are equal owing to $\nabla n^i = 0$:

$$\frac{\delta n^i}{\delta t} =: n^i_t + \underset{\sim}{W}^i \cdot \nabla n^i = n^i_t . \qquad (5.7)$$

The same applies, of course, to stationary values of n^e. This proves the validity of the above assertion.

The nonlinear K.P. equations with arbitrary $A(x)$, i.e. $\nabla A \not\equiv 0$, together with the boundary conditions of Sec. 4, are not only invariant to translations of y and t , they also remain invariant with respect to "translations with shear" of the form $y \to y + \eta(x)$, $\eta(x)$ arbitrary. Thus, for every solution $n^{i,e}(x,y,t)$, the functions $n^{i,e}(x, y+\eta(x), t+\tau)$ are also solutions. This invariance can be used for checking numerical solutions. By substituting a sum of Heaviside step functions for $\eta(x)$ a <u>discontinuous solution</u> is produced from an arbitrary, smooth solution. This proves again that the K.P. equations have discontinuous solutions, which ought to be eliminated for physical reasons, e.g. by suitable numerical methods or by adding diffusion terms.

In the special case $A_x = 0$ and $\overset{0}{n}_{xx} = 0$ a further invariance exists with respect to "pseudo - reflection" at the straight line $x = \frac{a}{2}$; i.e. for every solution $[\varrho(x,y,t)\ ,\ \varrho_t(x,y,t)]$ of eq. (3.5) (that satisfies the boundary conditions), the functions $[-\varrho(a-x,y,t), -\varrho_t(a-x,y,t)]$ also form such a solution. Antisymmetric initial conditions, viz.

$$\left.\begin{aligned} \varrho(x,y,0) + \varrho(a-x,y,0) &= 0, \\ \varrho_t(x,y,0) + \varrho_t(a-x,y,0) &= 0, \end{aligned}\right\} \qquad (5.8)$$

yield solutions that are antisymmetric at all times. Of course, periodicity of a solution $[\varrho, \varrho_t]$ in x and/or y is also conserved in time.

It would be desirable to derive constants of the motion from the invariance properties. This is not possible for want of a Lagrangian density producing the K.P. equations. It can, in fact, be readily proved that no polynomial function constructed from $n^{i,e}$ and first derivatives can be a Lagrangian density for the K.P. equations.

6. Necessary Conditions for Nonlinear Travelling Waves

Let us consider whether there exist solutions of the K.P. equations in the form of travelling waves that propagate in the y- direction, viz.

$$n^{i,e} = n^{i,e}(x, y - wt), \tag{6.1}$$

with $w=$ const. Only the special case with $\partial_x A = 0$, $\partial_x \nu_{ei} = 0$, and $\partial_x v^0 = 0$ is discussed, on the basis of eq. (3.5) for $\rho = n^i - n^e$. This equation now assumes the form

$$w^2 \rho_{yy} - K\rho_y + \nu_e \nu_i \rho$$

$$+ Aw(\rho_y \rho_{xy} - \rho_x \rho_{yy}) = 0, \tag{6.2}$$

with

$$K = (\nu_e + \nu_i)w + (\nu_e - \nu_i)v_0. \tag{6.3}$$

The boundary conditions at $x=0$ and $x=a$, eq. (4.5), yield $\rho = 0$ at these boundaries.

Multiplying eq. (6.2) by $2\rho_y$ yields

$$w^2(\rho_y^2)_y - 2K\rho_y^2 + \nu_e\nu_i(\rho^2)_y$$

$$+ Aw\left[(\rho_y^3)_x - (\rho_y^2 \cdot \rho_x)_y\right] = 0. \tag{6.4}$$

By integration over the domain of definition one obtains

$$\int_0^a dx \int_0^b dy \quad K \rho_y^{\,2} = 0. \tag{6.5}$$

This yields, for $K \neq 0$, only the trivial solution $\rho = \rho_y = 0$ representing the equilibrium $n^{i,e} = n^0$.

The case $K=0$ must be treated separately. Multiplying eq. (6.2) by ρ yields for $K=0$

$$W^2 (\rho\rho_y)_y - W^2 \rho_y^{\,2} + \nu_e \nu_i \rho^2$$

$$+ A W \left[(\rho\rho_y^{\,2})_x - (\rho\rho_x\rho_y)_y \right] = 0. \tag{6.6}$$

By integrating we obtain

$$\int_0^a dx \int_0^b dy \left(\nu_e \nu_i \rho^2 - W^2 \rho_y^{\,2} \right) = 0. \tag{6.7}$$

If one takes $\nu_i = 0$, the trivial solution $\rho = \rho_y = 0$ is again obtained. It follows that nonlinear waves are only possible for $K=0,\ \nu_e \nu_i \neq 0$ at most. It was not possible to give a proof of existence or construct solutions for this case. This result is in contrast with the disparate cases of LAQUEY et al. (1975) and COHEN et al. (1976). Their equations differ essentially from the K.P. equations used here in that they include Landau damping and $A_x \neq 0$ and use various approximations; unlike the present result, their equations do allow nonlinear travelling waves with $W = -v_0$ in the case $\nu_i = 0$.

7. Dimensional Analysis: Parameter Dependence of the Anomalous Diffusion Coefficient

Let us write eqs. (3.2) and (3.3) in the form

$$\tilde{n}^i_t + \nu_i \tilde{n}^i - v_0 \rho_y + A\left(\tilde{n}^i_x \tilde{n}^e_y - \tilde{n}^i_y \tilde{n}^e_x\right) = 0, \quad (7.1)$$

$$\tilde{n}^e_t + \nu_e \tilde{n}^e - v_0 \rho_y + A\left(\tilde{n}^i_x \tilde{n}^e_y - \tilde{n}^i_y \tilde{n}^e_x\right) = 0, \quad (7.2)$$

with $\rho = n^i - n^e$, $\tilde{n}^{i,e} = n^{i,e} - n^0$, and v_0 being defined as after eq. (3.8). By using the units ν_e^{-1}, a, a, and n^0 for the variables t, x, y, and $\tilde{n}^{i,e}$, including ρ, one obtains the dimensionless equations

$$\mu^i_\tau + \frac{\nu_i}{\nu_e}\mu^i - \frac{v_0}{\nu_e a}\sigma_\eta + \frac{A n^0}{\nu_e a^2}\left(\mu^i_\xi \mu^e_\eta - \mu^i_\eta \mu^e_\xi\right) = 0, \quad (7.3)$$

$$\mu^e_\tau + \mu^e - \frac{v_0}{\nu_e a}\sigma_\eta + \frac{A n^0}{\nu_e a^2}\left(\mu^i_\xi \mu^e_\eta - \mu^i_\eta \mu^e_\xi\right) = 0, \quad (7.4)$$

where τ, ξ, η, $\mu^{i,e}$, σ are the dimensionless substitutes for t, x, y, $\tilde{n}^{i,e}$, ρ. The boundary conditions require that $\mu^{i,e}$ and σ be periodic in η with, say, the period $\eta_0 = \frac{b}{a} = 1$; and that $\mu^{i,e}_\eta = 0$ at the walls $\xi = 0$ and $\xi = 1$. Hence the solutions of eqs. (7.3), (7.4) depend on the variables τ, ξ, η, on the parameters

$$\left.\begin{aligned} c_1 &= \nu_i / \nu_e \,, \\ c_2 &= \frac{v_0}{\nu_e a} \sim \frac{A n^0}{\nu_e a^2} \,, \end{aligned}\right\} \tag{7.5}$$

and on the initial conditions.

Let us now consider the anomalous diffusion coefficient. According to eq. (3.10) the diffusion coefficient is given by

$$D =: \frac{\Gamma^x}{n_x^0} \approx - \frac{A}{\nu_e n_x^0} \langle \rho_t \cdot \rho_y \rangle \,, \tag{7.6}$$

or

$$D \approx A n^0 \langle \sigma_\tau \cdot \sigma_\eta \rangle \,. \tag{7.7}$$

If the pointed brackets are now re-interpreted as an average over x, y, and t for large times, and if it is assumed that an asymptotic value of D is attained for $t \to \infty$ that is independent of the initial conditions, then it follows that

$$D = a v_0 \cdot g_1 (c_1, c_2) \,, \tag{7.8}$$

where g_1 is an undetermined function. Other possible forms of eq. (7.8) are, for example,

$$D = \frac{v_0^2}{\nu_e} g_2 (c_1, c_2) \tag{7.9}$$

or

$$\mathcal{D} = \nu_i a^2 \cdot g_3(c_1, c_2). \tag{7.10}$$

Equation (7.9) exhibits the K.P. scaling in the dimensional factor, while eq. (7.10) refers to creation and annihilation of the trapped ions by collisions (SAISON and WIMMEL, 1975; WIMMEL, 1976). In terms of experimental parameters, viz. a, B, N^P, T, δ_0, and for a given choice of ions and of T_i/T_e one has $c_1 = \text{const}$ and

$$c_2 \propto \frac{\delta_0^3 \, T^{5/2}}{a^2 B N^P (1-\delta_0)}. \tag{7.11}$$

If, in particular, one assumes g_3 to represent a power law, viz. $g_3 \sim c_2^\alpha$, then the scaling law for $\mathcal{D}$ will read

$$\mathcal{D} \propto \frac{a^2 N^P}{\delta_0^2 T^{3/2}} \cdot \left[\frac{\delta_0^3 \, T^{5/2}}{a^2 B N^P (1-\delta_0)} \right]^\alpha , \tag{7.12}$$

with α undetermined. For $\alpha = 1$ and $\alpha = 2$ Bohm scaling and Kadomtsev-Pogutse scaling are recovered. Equations (7.8) to (7.10) can be used for checking numerical results.

8. Numerical Computations

Equations (2.1) to (2.8), with $\partial_x A = \partial_x^2 n^0 = 0$ and $\nu_{i,e} =$ const , together with the boundary conditions of eq. (4.5), were numerically solved in the range $0 \leqq x \leqq a,\ 0 \leqq y \leqq b = a,\ t \geqq 0$. From the solutions the diffusion coefficient D with respect to the gradient of the trapped equilibrium density $n^0(x)$, viz.

$$D(x,t) = -\frac{1}{b}\int_0^b dy \left(\frac{n^i + n^e}{2}\right) v^x / \nabla n^0 , \tag{8.1}$$

was determined. The numerical calculations use an explicit version of the Carlson method (see RICHTMYER, 1957). Most runs were performed with a 60 x 60 quadratic grid $(\Delta x = \Delta y)$; some calculations with a 30 x 30 grid and test runs with 70 x 70 up to 110 x 110 grids were also performed. The equilibrium used was of the form

$$n^0(x) = n^0(0)\left(1 - \frac{x}{a}\right), \tag{8.2}$$

with $\delta_0 =$ const. Hence, N^p and T are also known functions of x. The numerical values of N^p and T given below are the values at $x = 0$. The collision frequencies $\nu_{i,e}$ are calculated from these values on the axis. The formula

$$\nu_{i,e} = \nu_{i,e}^{COUL}\left(\frac{\pi/2}{\arcsin \delta_0}\right)^2 \tag{8.3}$$

was used instead of $\nu_{i,e} = \nu_{i,e}^{COUL} / \delta_0^2$. The following boundary conditions were used:

$$n^{i,e}(x_W, y, t) = n^0(x_W), \tag{8.4}$$

for $x_W = 0$ and $x_W = a$, as well as periodicity in y, with the period $b = a$.

Generally, the initial perturbations were of the form

$$n^{i,e} = c^0 x(a-x) \sum_{m=1}^{m_0} \frac{1}{m} \left[\tilde{A} \cos(m\varphi + \theta) \pm \cos m\varphi \right], \tag{8.5}$$

with $\varphi = 2\pi y/b$, $c^0 = 2 \cdot 10^7$, $m_0 = 4$. Other values of m_0 were also used. The constants $\tilde{A}$ and θ were determined in such a way that $m = m_0$ gave a purely growing term according to the linearized theory. The time step Δt was variable and was determined as

$$\Delta t = \min(\Delta t_1, \Delta t_2, \Delta t_3, \Delta t_4), \tag{8.6}$$

with $\Delta t_1 = 2\,\mu\mathrm{sec}$, $\Delta t_2 = (10\nu_e)^{-1}$, $\Delta t_3 = \Delta x/(1.1 \max|v^x|)$, $\Delta t_4 = \Delta y/(1.1 \max|v^y|)$. Replacing Δt by $\Delta t/5$ in one run did not appreciably alter the time asymptotic value of the diffusion coefficient: D decreased by only about 10 %.

9. Numerical Results

We now present the numerical results. As a parameter, the critical wavelength $\lambda_c = 2\pi v_0 / (\nu_e \sqrt{5})$ is used (WIMMEL, 1976/1). For $\lambda_c > a$ the diffusion coefficient D does not approach an asymptotic value. Rather does D at $x = \frac{a}{2}$ fluctuate in time between zero and a maximal value of the order of $D_{K.P.}$. One-dimensional Fourier analysis in the y-direction shows that most of the energy resides in the $m=1$ and $m=0$ modes. This parameter range is close to the limit of validity of the theory, where magnetic drifts become important, and a transition to the collisionless trapped-ion mode occurs (KADOMTSEV and POGUTSE, 1970, 1971). In an intermediate range, $a/2 > \lambda_c > a/4$, fluctuations of D in time become smaller. The fluctuating asymptotic state is reached, on the average, after $10\ ms$, in the range of parameters we considered. Again, most of the energy resides in the $m=1$ and $m=0$ modes.

In the regime of small-scale convection, i.e. $\lambda_c < \frac{a}{4}$, the diffusion coefficient in most runs assumes a constant asymptotic value after about 5 to 10 ms. Between the initial phase of linear growth and the asymptotic phase there is a strongly nonlinear phase in which D may exceed the asymptotic value by a large factor and, in addition, may strongly oscillate (see Fig. 1). The final state is characterized by an azimuthal mode number m $\geqq$ 1 in which, again except for $m=0$, most of the energy resides. For this range a diagram of equipotential contours, showing also the direction of the $\underset{\sim}{E} \times \underset{\sim}{B}$ drift, is given, with $m_{final} = 1$ (see Fig. 2).

In agreement with analytical results the potential shows a dipole effect. In this case as well as for larger values of m_{final} no indication of a disordered, turbulent state is found; rather an ordered wave pattern prevails. The one-dimensional Fourier transforms of E_y and E_x in the y and x-directions yield the 4 energy spectra $W_y(m,x)$, $W_x(m,x)$, $\tilde{W}_y(n,y)$, $\tilde{W}_x(n,y)$, where m and n are the mode numbers in the y and x-directions, respectively. While, in a case with $m_{final} = 2$, W_y is strongly peaked at $m=2$, W_x at $m=0$ and 2, $\tilde{W}_x$ and $\tilde{W}_y$ are smooth spectral distributions with respect to n. Of course, the kinetic energy density of the drift motion is much larger than the electrostatic energy density, the ratio between the two being of the order of $c^2/v_A^2 \gg 1$, with v_A = Alfvén speed. But for our purpose it is sufficient to consider the electrostatic energy spectrum alone.

A peculiar phenomenon may occur for carefully selected parameters in the transition region between different values of the final m-number (see Fig. 3). In the example, first a metastable state with $m=4$ is reached; then, after 15msec, a sudden jump to a final state $m=2$ occurs. By this transition, the diffusion coefficient is enlarged by a factor of two.

In Figs. 4 to 6 we show the dependence of several dimensionless versions of the anomalous diffusion coefficient on the dimensionless quantity

$$m_{marg} = \frac{a}{2\pi v_0}\sqrt{\nu_e \nu_i} \tag{9.1}$$

that describes the equilibrium state considered, and that is proportional to a/λ_c. Because the original calculations were carried out varying the dimensional parameters B, T, N^P, a, δ_0 separately, the results reduced to dimensionless form show that the quantity m_{marg} is the only equilibrium parameter that matters for the diffusion coefficient. Figure 4 shows that the diffusion is roughly Bohm-like since the quantity $a\vartheta_0$ is proportional to D_{Bohm}; Fig. 5 proves that the diffusion is generally stronger than according to K.P.; Fig. 6 compares the diffusion to trapped ion creation and annihilation by ion collisions. All three figures demonstrate a sawtooth structure of the diffusion curves that comes about by the differing values of the final mode number, m_{final} (Fig. 7), and by the fact that the global scaling of D differs from the "local" scaling valid for a constant value of m_{final}.

In order to prove that the results are independent of the number of grid intervals, this number (NX = NY) was varied, for a particular equilibrium, between NX = 60 up to NX = 110. Figure 8 shows the resulting diffusion coefficient and final mode number, which are both fairly independent of NX. In addition, the initial conditions were varied in two different ways. First, the quantity m_0 of Sec. 8 was varied between 1 and 10 (Fig. 9, solid line); second, monochromatic initial conditions, i.e. $m_{init} = m_o$, m_o from 1 to 10, were used (Fig. 9, dashed line). Figure 9 demonstrates that the diffusion coefficient does not vary too much with this set of initial conditions, while the final mode number varies to a greater extent, particularly so in the case of monochromatic initial excitation; as might be expected.

The fact that the final states contain a large-amplitude, $m = 0$ Fourier component points to a possible saturation mechanism, i.e. modification of the equilibrium density profile of the trapped ions. Here the question arises whether it is the profile modification averaged over y or the local profile modification, e.g. the maximum deviation from the equilibrium, that counts for saturation. In Fig. 10 the radial density profile, averaged over y, of the trapped ions is shown for the time-asymptotic state. It is seen that the profile is far from forming a plateau. However, the maximum local trapped-ion density has a deviation from the equilibrium density that is 3 to 4 times greater than the average deviation in this case. (This fact has not been diagnosed directly; rather is it deduced by comparing average and maximum values of the electric potential). Hence, it appears that it is the maximum density perturbation that approximately satisfies the mixing length condition of saturation (WIMMEL, 1976/1) viz.

$$|K_x| \cdot |\tilde{n}^i|_{max} \sim |\nabla n^0| . \tag{9.2}$$

The reason, in terms of the mixing length model (WIMMEL, 1976/1), that the diffusion is nevertheless larger than according to K.P. (Fig. 5) seems to be that rather than having $|K_x| \approx |K_y|$ as is postulated by K.P., we find

$$|K_x|_{av} \ll |K_y|. \tag{9.3}$$

In fact, the ansatz

$$|K_x|_{av} \propto \sqrt{2\pi |K_y| / a} \tag{9.4}$$

reproduces Bohm-type diffusion, as is explained in the next section.

If one considers, instead, a picture of mode-mode interaction, then, according to linearized theory, the m = 0 modes provide for damping, while $m_{final} = m_1$ and its harmonics give rise to growth. Hence, if a conserved, energy-like quantity existed, this quantity were to flow from higher to lower azimuthal wave numbers m. This flow direction is opposite to the one implied by KADOMTSEV and POGUTSE (1970, 1971) and explicitly mentioned by LAQUEY et al. (1975). However, because the $\underset{\sim}{E} \times \underset{\sim}{B}$ drifts, when they vary in time, couple to the reservoir of internal energy, no useful energy conservation theorem can be formulated for the nonlinear K.P. equations, that is, in terms of the macroscopic variables n^i, n^e, Φ, $\underset{\sim}{E}$, and $\underset{\sim}{\vartheta}$ alone which enter the K.P. equations. Notice that this difficulty refers not to the collision terms, but rather to the convection terms of the K.P. equations.

10. Discussion

Our results are important mainly because they stem from the first successful 2-D computations made so far, and that they contradict the earlier claims by KADOMTSEV and POGUTSE (1970, 1971). In the following, we shall discuss several points that refer to the question how reliable our results probably are.

First of all, it is plausible that the diffusion depends on the spatial extent (coherence length) of the perturbations in the x - direction. Our calculations, by specializing to $\nabla v_0 = 0$, probably maximize this radial coherence length and, hence, also the diffusion coefficient. This can be made plausible by considering a mixing length ansatz (WIMMEL, 1976/1), whereby

$$D \sim - \frac{A \nu_e K_y \omega}{K_x^2 \left(\nu_e^2 + \omega^2 \right)} \partial_x n^0 . \tag{10.1}$$

It is seen that Bohm scaling, consistent with the numerical results, is obtained by a special choice of the average $|K_x|$ namely by taking the effective coherence length

$$\ell_x =: 2\pi / |K_x| \propto \sqrt{2\pi a / |K_y|} , \tag{10.2}$$

and by choosing $|\omega| \approx |\omega_0| \approx \nu_e$, sign $(\omega/\omega_0) = -1$. Such a value of ℓ_x is in agreement with the fact that the numerical solutions exhibit broad K_x- spectra. However, for $\nabla v_0 \neq 0$ both ℓ_x and D will possibly be reduced because the dominating ω and/or the dominating k_y could become x- dependent and, thus, impair wave coherence.

A second point concerns particle detrapping. The time-asymptotic plasma states of the computations satisfy a rough condition for electrostatic detrapping being absent (LAQUEY et al., 1975), viz.

$$|e\Phi/T| < \delta_0^2 . \tag{10.3}$$

However, at short times, the spatial maximum of the potential goes through a maximum value that may violate eq. (10.3). Therefore it will be desirable to modify the K.P. equations to include detrapping effects and repeat the numerical calculations. It could well be that the final plasma states will be nearly the same as without this modifications; but this is not known at present.

A third point concerns the additional occurrence of the ion diamagnetic branch of the dissipative trapped-ion instability (TANG et al., 1976). In special cases such that the magnetic particle drift can be assumed to be destabilizing for ions of arbitrary pitch angle (condition for the magnetic shear: $q'r/q \sim 1$) there are apparently regimes in the parameter space where the ion diamagnetic modes dominate in terms of linear growth rates. Such modes are not taken into account in the K.P. fluid equations.

A fourth point concerns the comparison of our calculations with several 1-D computations by other authors (LAQUEY et al., 1975, and COHEN et al., 1976). These authors have reduced the K.P.

equations to one spatial dimension by using a number of approximations. By this device the character of the K.P. equations is altered so much as to even lack the fundamental property of saturation, which the original K.P. equations possess (see Sec. 5). As a consequence, additional damping must be added, and it is Landau damping that has been chosen for this purpose. But, for $\eta_i > \frac{2}{3}$ Landau damping is <u>negative</u>, i.e. <u>destabilizing.</u> Therefore, the 1-D theory was not evaluated for the important cases with $\eta_i > \frac{2}{3}$. Further critical points are the following:

a) The 1-D theory neglects the aspect of wave coherence in the x - direction. However, our 2-D results show that the time-asymptotic diffusion coefficient can be influenced by the x- dependence of the initial conditions.

b) At large perturbation amplitudes the validity of the Landau-damping formula is uncertain.

c) The 1-D results of Princeton for the diffusion coefficient depend in an extremely sensitive fashion on the equilibrium parameters. Hence, the <u>practical value</u> of those results appears to be questionable.

The last point will be illustrated by giving a <u>quantitative</u> argument. The anomalous diffusion coefficient D given by COHEN et al. (1976), eq. (48), when corrected according to an earlier version of the paper (see MATT-1259, 1976) has the form

$$D \propto \frac{r_n^2 \, \varepsilon^{8.5} \, T^{10.5}}{q^6 \, R^6 \, n^5} \left(1 - \frac{3}{2}\eta_i\right), \qquad (10.4)$$

where the symbols have their usual meaning (explained in the reference cited). In order to obtain eq. (10.4) from the Cohen paper, one must insert the formula for $D_{K.P.}$ in the formula for $D/D_{K.P.}$ given there. This diffusion coefficient then does not depend or the magnetic field B, but very large exponents operate on most of the other quantities. For instance, increasing T by a factor of 2 increases D by a factor greater than 1000. This does not agree with our 2-D results. In these an opposite tendency is effective, namely the dependence of D on the equilibrium parameters is much weaker than according to KADOMTSEV and POGUTSE (1970, 1971) and, *a fortiori,* than according to COHEN et al. (1976).

From what has been said we think that our 2-D analysis is superior to the 1-D computations mentioned. It presents no problem to insert a Landau damping term and/or other damping terms in our equations. But, contrary to the 1-D approximation, our 2-D solutions saturate already without Landau damping, and they better represent the extended type of modes (GLADD and ROSS, 1973) which we expect to dominate anomalous diffusion.

11. Summary

We have presented numerical results on nonlinear saturation and anomalous diffusion due to unstable, dissipative trapped-ion modes. This has been the first successful 2-D treatment of this problem, including boundary effects and time-dependent behavior, starting from given initial density distributions. Several effects, e.g. neoclassical diffusion, Landau damping, viscosity, finite gyroradii, have not been included so far.

The main numerical results are: At large times, saturation occurs, and in the prevailing cases the diffusion coefficient D approaches a time-independent value. Usually, an ordered wave pattern evolves, with only a few azimuthal wave numbers visible, viz. $m = 0$ and $m = m_1$ depending on the equilibrium parameters. Harmonics of m_1 are also present, but with much lower intensities. A turbulent state, with many modes excited, and showing a stochastic behaviour, is not found at all. The diffusion coefficient D scales nearly Bohm-like and, generally, is larger than according to the K.P. formula (KADOMTSEV et al., 1970, 1971). It appears that in a mixing-length model (WIMMEL, 1976/1) the result $D > D_{K.P.}$ can be understood by the fact that rather than $|K_x| \approx |K_y|$ one has

$$|K_x|_{av} \ll |K_y| , \tag{11.1}$$

while the condition for the maximum saturation amplitude is unaltered (WIMMEL, 1976/1):

$$|K_x|_{av} \cdot |\tilde{n}^i|_{max} \sim |\nabla n^0|. \qquad (11.2)$$

When the equilibrium parameters are varied, there exist small transition regions in parameter space where the azimuthal wave number that shows up at late times, $m_{final} = m_1$, tends to jump to another integer value. In these regions solutions behave somewhat irregular, as explained in Sec. 9, but these "quantum effects" do not affect the overall picture.

The main analytical results are: The boundary conditions forbid true wall losses, but allow anomalous diffusion in the plasma volume. Dimensional analysis gives useful information on the scaling properties of the anomalous diffusion coefficient. Special solutions and bounds of the general solutions are obtained. Invariance properties of the K.P. equations are considered, and necessary conditions for the existence of travelling waves are derived.

After we had completed this paper, additional work on the trapped ion mode driven by ion magnetic drift (see Sec. 10) came to our attention (TAGGER et al., 1977).

Acknowledgment - We thank Dietrich Lortz for a valuable discussion.

"This work was performed under the terms of the agreement on association between the Max-Planck-Institut für Plasmaphysik and EURATOM".

References

COHEN B.I., KROMMES J.A., TANG W.M., and ROSENBLUTH M.N. (1976), Nucl. Fusion 16, 971.

COPPI B. and REWOLDT G. (1976) Advances in Plasma Physics (SIMON A. and THOMPSON W.B., Eds.) Vol. 6., p. 421 - 585. John Wiley & Sons.

DOBROWOLNY M. and NOCENTINI A. (1973) Nucl. Fusion 13, 629.

DOBROWOLNY M. (1974) Plasma Physics 16, 996.

DOBROWOLNY M. (1974) Nucl. Fusion 14, 599.

DOBROWOLNY M. and ROSS D.W. (1975) Phys. Fluids 18, 717.

GLADD N.T. and ROSS D.W. (1973) Phys. Fluids 16, 1706.

GREEN B.J., MARTY D., PFIRSCH D., SAISON R. and WIMMEL H.K. (1974) Plasma Physics and Controlled Nuclear Fusion Research (Proc. 5th Conf., Tokyo), paper IAEA - CN - 33/A 14-1. International Atomic Energy Agency.

JABLON C., LAVAL G., and PELLAT R. (1971) Phys. Rev. Lett. 27, 83.

JABLON C.J. (1972) Phys. Rev. Lett. 28, 880.

KADOMTSEV B.B. and POGUTSE O.P. (1967) Sov. Phys. JETP 24, 1172.

KADOMTSEV B.B. and POGUTSE O.P. (1970) Reviews of Plasma Physics (LEONTOVICH M.A., Ed.) Vol. 5, p. 249. Consultants Bureau, New York.

KADOMTSEV B.B. and POGUTSE O.P. (1971) Nucl. Fusion 11, 67.

LAQUEY R.E., MAHAJAN S.M., RUTHERFORD P.H., and TANG W.M. (1975) Phys. Rev. Lett. 34, 391.

PFIRSCH D., SAISON R., WIMMEL H.K. (1974) JET Workshop (Culham), Paper B.1. Culham Laboratory.

RICHTMYER R.D. (1957) Difference Methods for Initial-Value-Problems. Interscience, New York,

ROSENBLUTH, M.N., ROSS D.W., and KOSTOMAROV D.P. (1972) Nucl. Fusion 12, 3.

SAGDEEV R.Z. and GALEEV A.A. (1968) Sov. Phys. Doklady 13, 562.

SAISON R. and WIMMEL H.K. (1975) Waves and Instabilities in Plasmas (2nd Int. Congr., Innsbruck) Paper P.3. University of Innsbruck.

TAGGER M., LAVAL G., and PELLAT R. (1977) Nucl. Fusion 17, 109.

TANG W.M. (1973) Nucl. Fusion 13, 883.

TANG W.M. (1974) Phys. Fluids 17, 1249.

TANG W.M., ADAM J.C., and ROSS D.W. (1976) Residual Trapped-Ion Instabilities in Tokamaks. Preprint. Princeton Univ. and Univ. of Texas at Austin.

WIMMEL H.K. (1975) Controlled Fusion and Plasma Physics (Proc. 7th Europ. Conf., Lausanne) Vol. 1 p. 121.

WIMMEL H.K. (1976) Plasma Physics 18, 321.

WIMMEL H.K. (1976) Plasma Physics 18, 693.

Figure Captions

Fig. 1. - Diffusion coefficient D vs. time t, normal situation.

Fig. 2. - Example of equipotential contours at late times, for $m_{final} = 1$. The arrows give the direction of the $\underset{\sim}{E} \times \underset{\sim}{B}$ drift velocity.

Fig. 3. - Diffusion coefficient vs. time, special situation, equilibrium parameters in a transition region between different values of m_{final}.

Fig. 4. - Bohm-type scaling of the anomalous diffusion coefficient, (D/av_o) vs. m_{marg}.

Fig. 5. - Comparison of the anomalous diffusion coefficient with the Kadomtsev - Pogutse formula: $D/D_{K.P.}$ vs. m_{marg}.

Fig. 6. - Dimensionless diffusion coefficient $(D/\nu_i a^2)$ vs. m_{marg}.

Fig. 7. - Final dominant mode number m_{final} vs. m_{marg}.

Fig. 8. - Test of validity of calculations. Diffusion coefficient D vs. the number of grid intervals, NX = NY.

Fig. 9. - Another test, involving variation of initial conditions. Diffusion coefficient vs. parameter m_o describing the initial spectrum (see main text).

Fig. 10. - Average radial density profile of the trapped ions (solid line), and equilibrium density profile (broken line).

Fig. 1

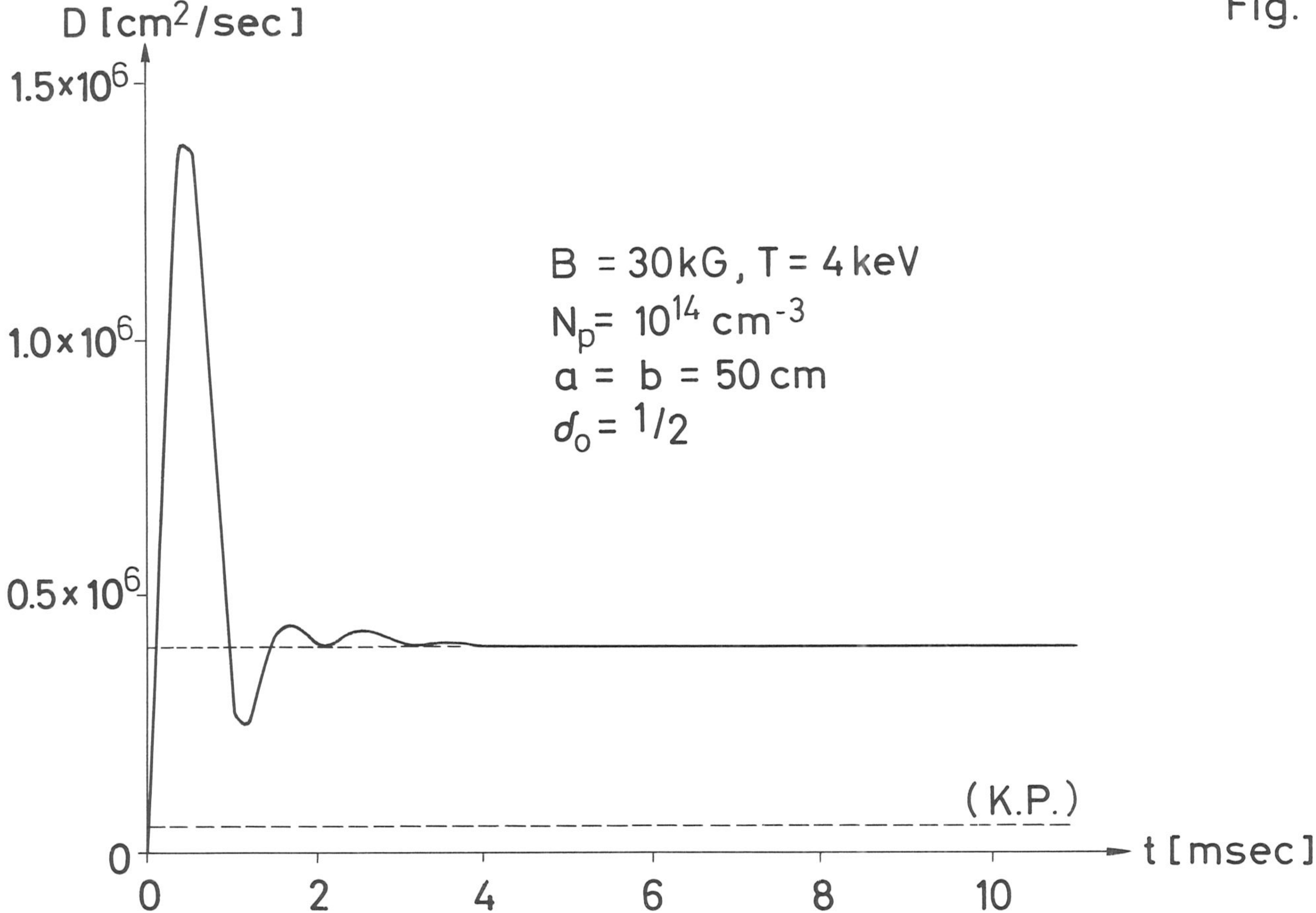

Diffusion Coefficient in Time

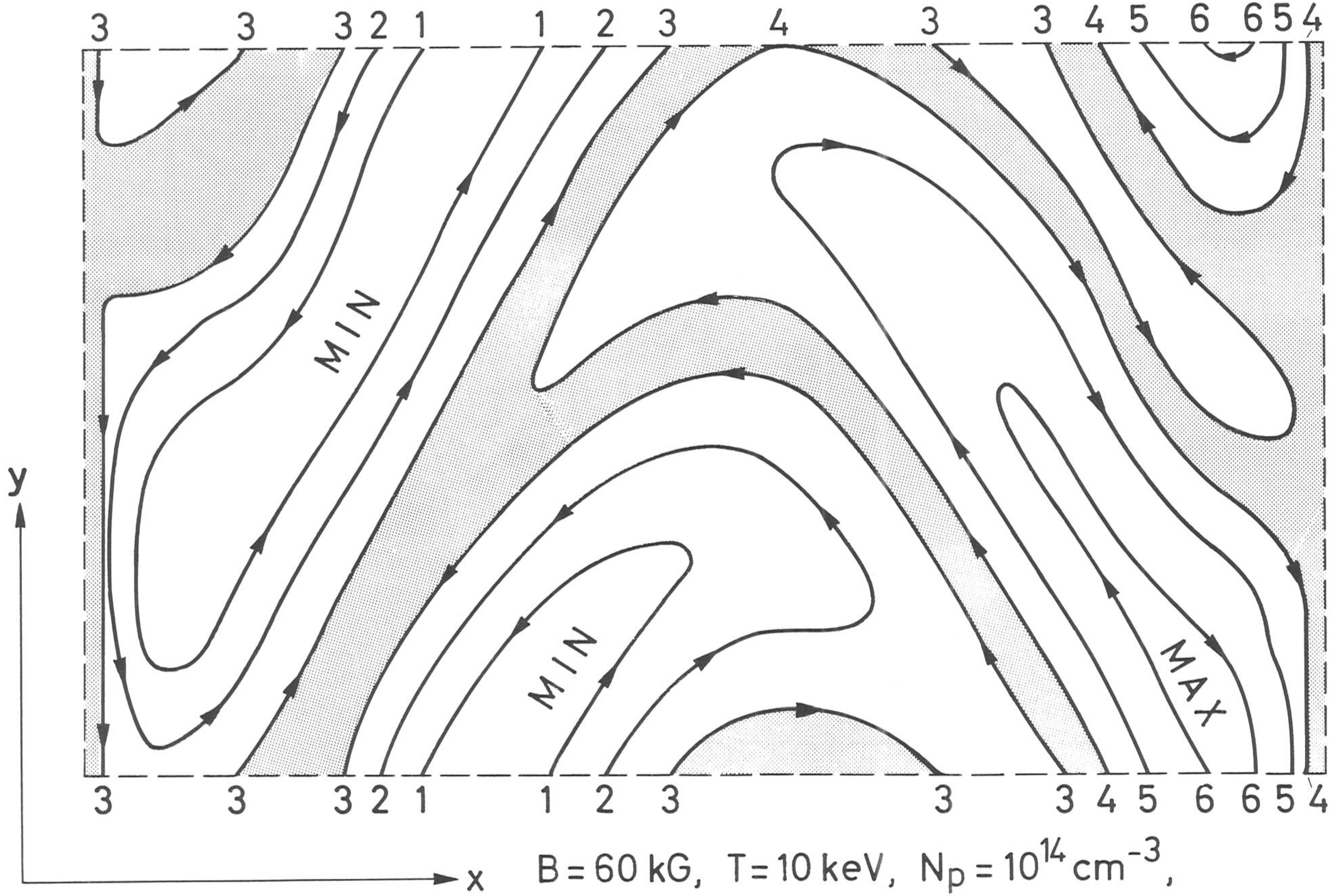

$B = 60\,\mathrm{kG}$, $T = 10\,\mathrm{keV}$, $N_p = 10^{14}\,\mathrm{cm}^{-3}$,

$a = b = 50\,\mathrm{cm}$, $\delta_o = 1/2$, $t = 20\,\mathrm{ms}$

Fig. 3

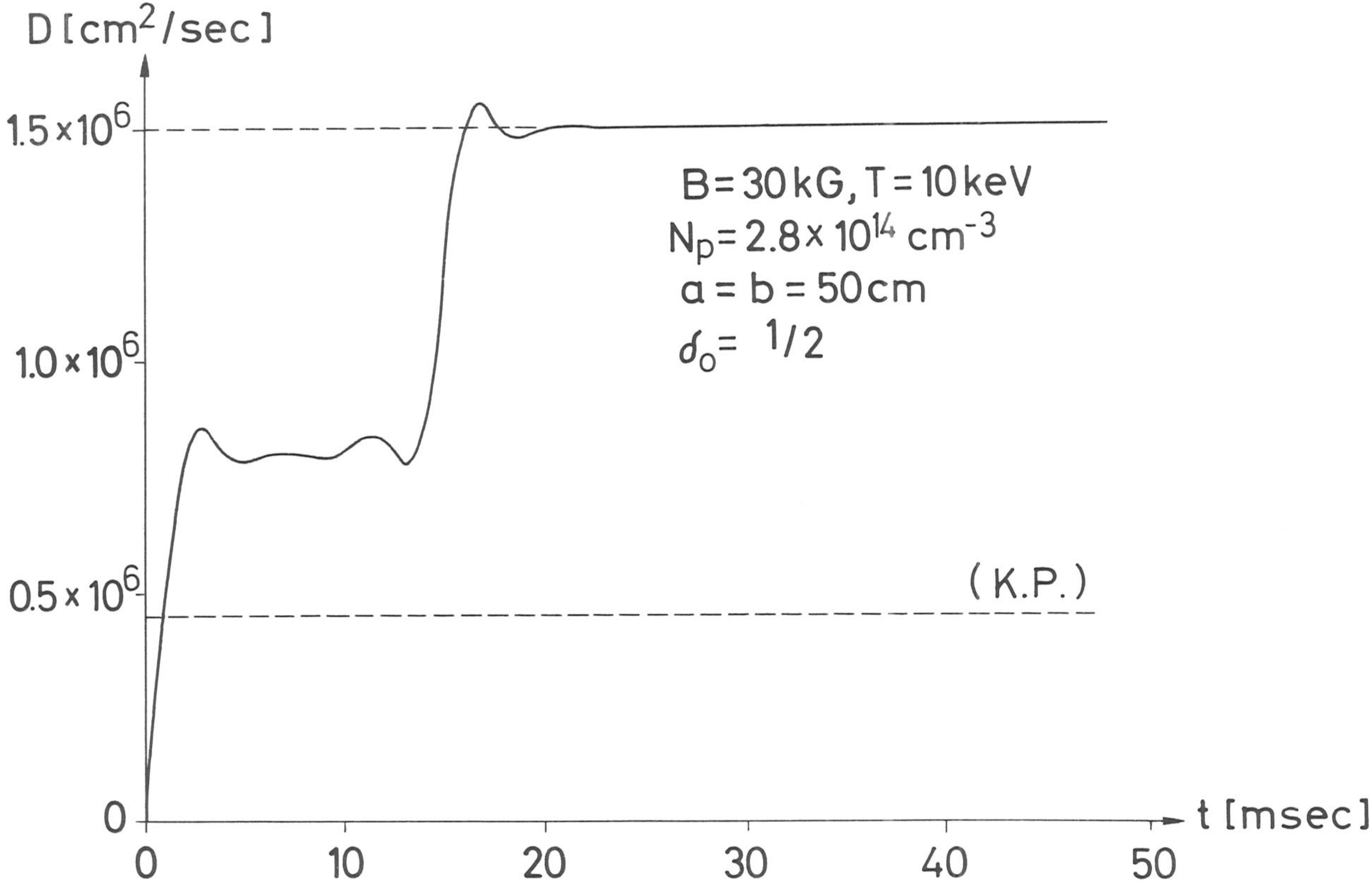

Diffusion Coefficient in Time

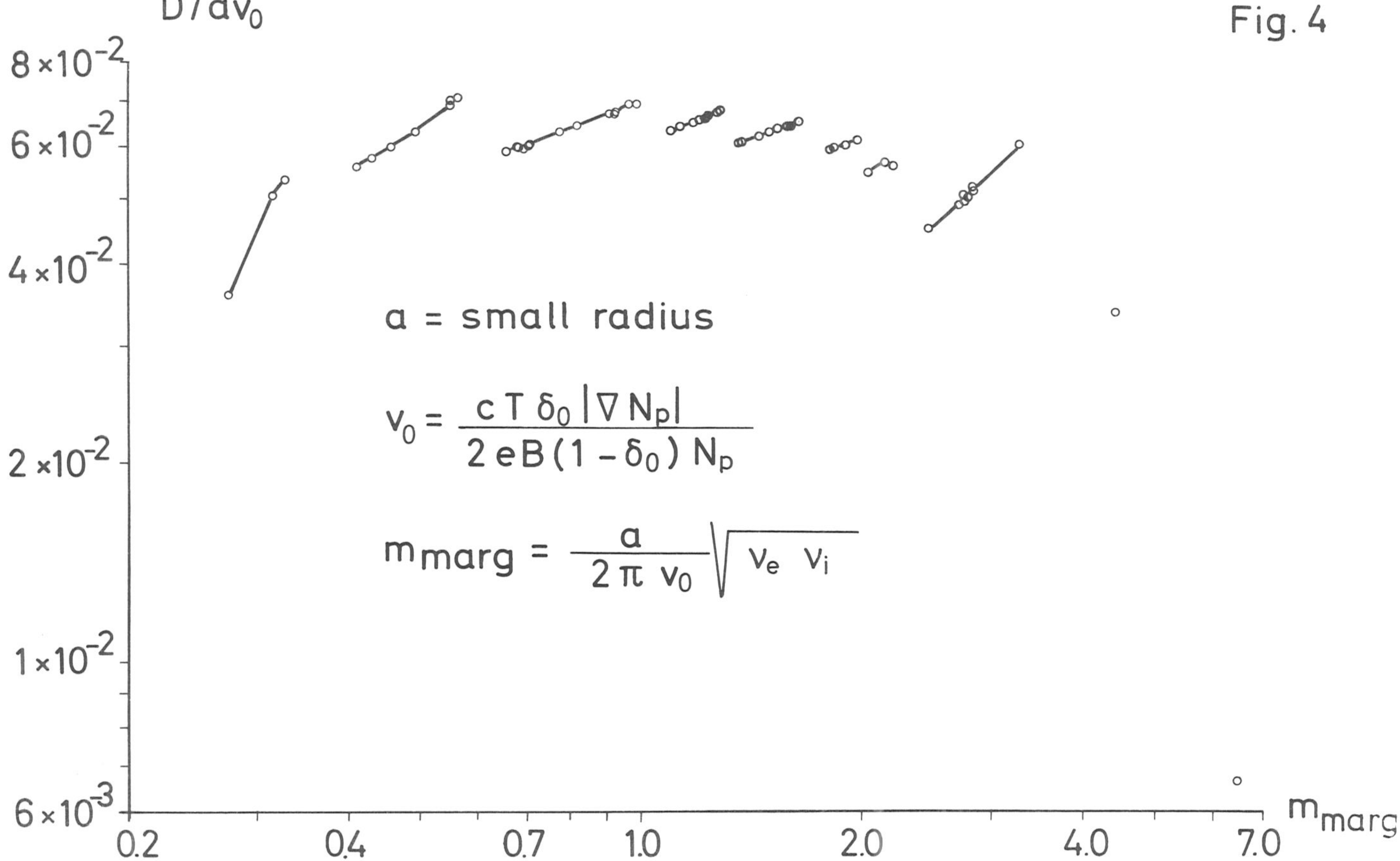

D/av_0
8×10^{-2}
6×10^{-2}
4×10^{-2}
2×10^{-2}
1×10^{-2}
6×10^{-3}
0.2
0.4
0.7
1.0
2.0
4.0
7.0
m_{marg}
a = small radius
$$v_0 = \frac{c\,T\,\delta_0\,|\nabla N_p|}{2\,e\,B\,(1-\delta_0)\,N_p}$$
$$m_{marg} = \frac{a}{2\pi\,v_0}\sqrt{\nu_e\ \nu_i}$$

Fig. 4

Fig. 5

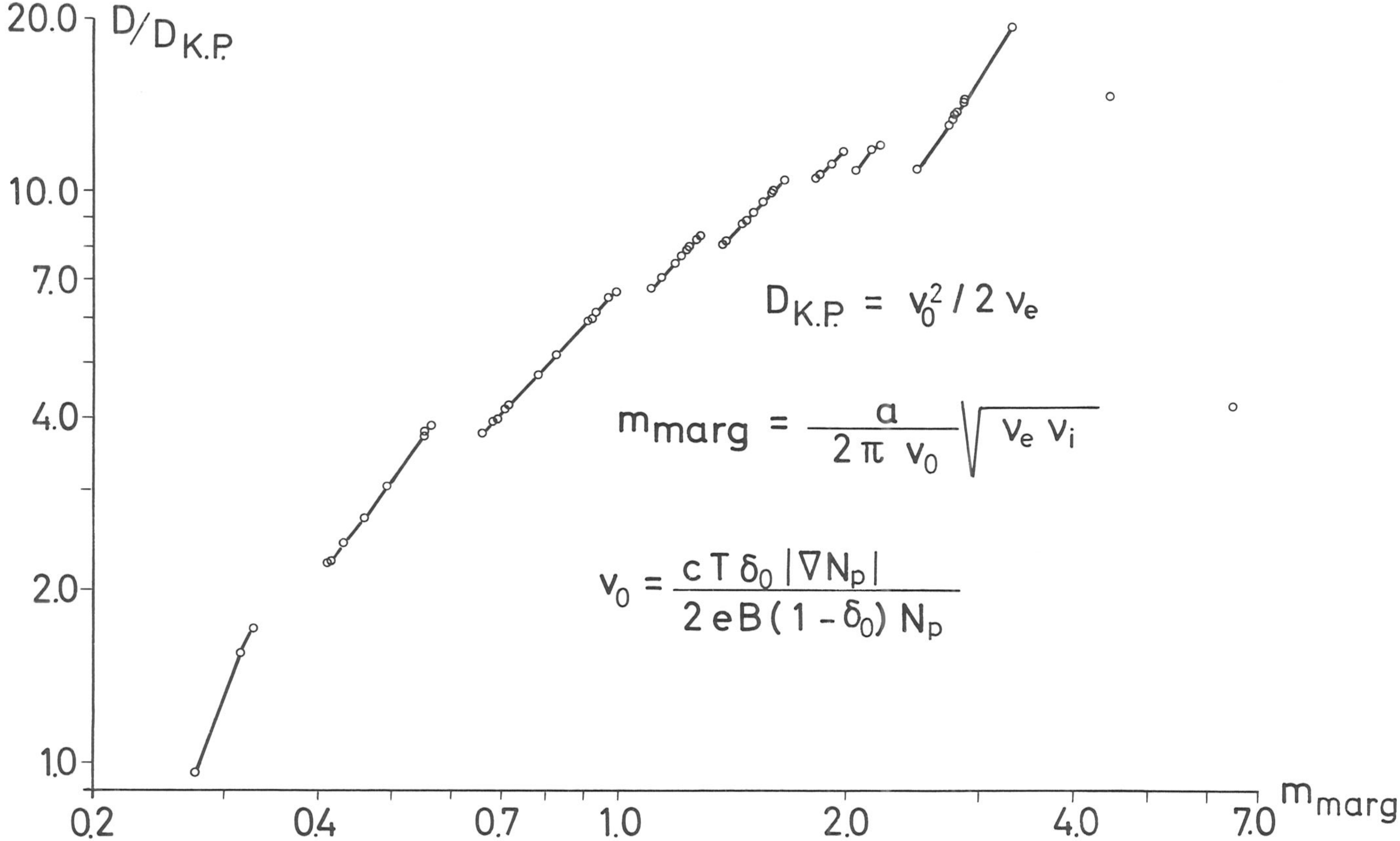

20.0
10.0
7.0
4.0
2.0
1.0
D/D K.P.
0.2
0.4
0.7
1.0
2.0
4.0
7.0
m marg
$D_{K.P.} = \nu_0^2 / 2\,\nu_e$
$m_{marg} = \frac{a}{2\pi\,\nu_0}\sqrt{\nu_e\,\nu_i}$
$\nu_0 = \frac{c\,T\,\delta_0\,|\nabla N_p|}{2\,e\,B\,(1-\delta_0)\,N_p}$

Fig. 6

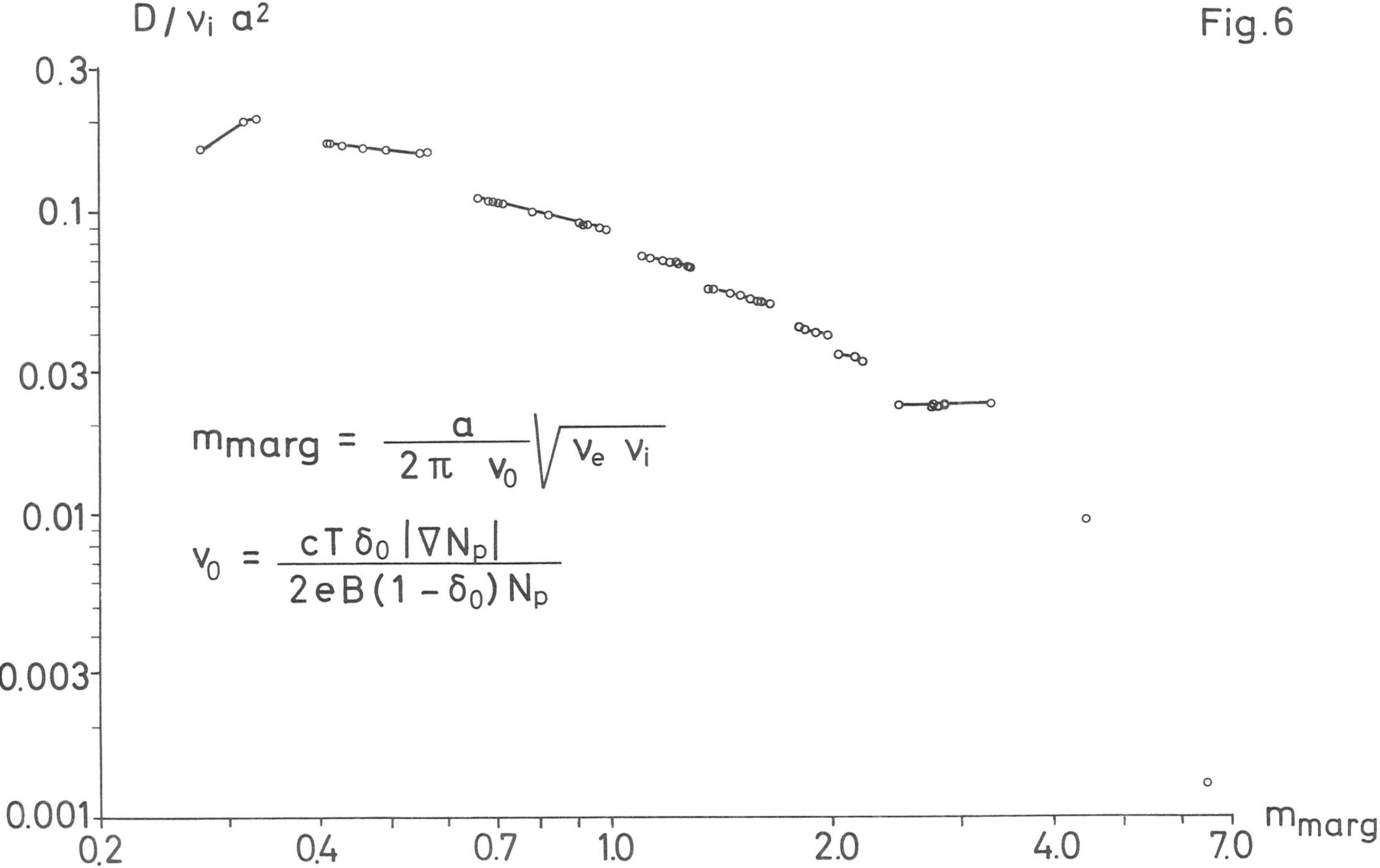
D / ν_i a²
0.3
0.1
0.03
0.01
0.003
0.001
0.2
0.4
0.7
1.0
2.0
4.0
7.0
m_marg
m_marg = a / (2π ν_0) √(ν_e ν_i)
ν_0 = cT δ_0 |∇N_p| / (2eB(1 − δ_0) N_p)

Fig. 7

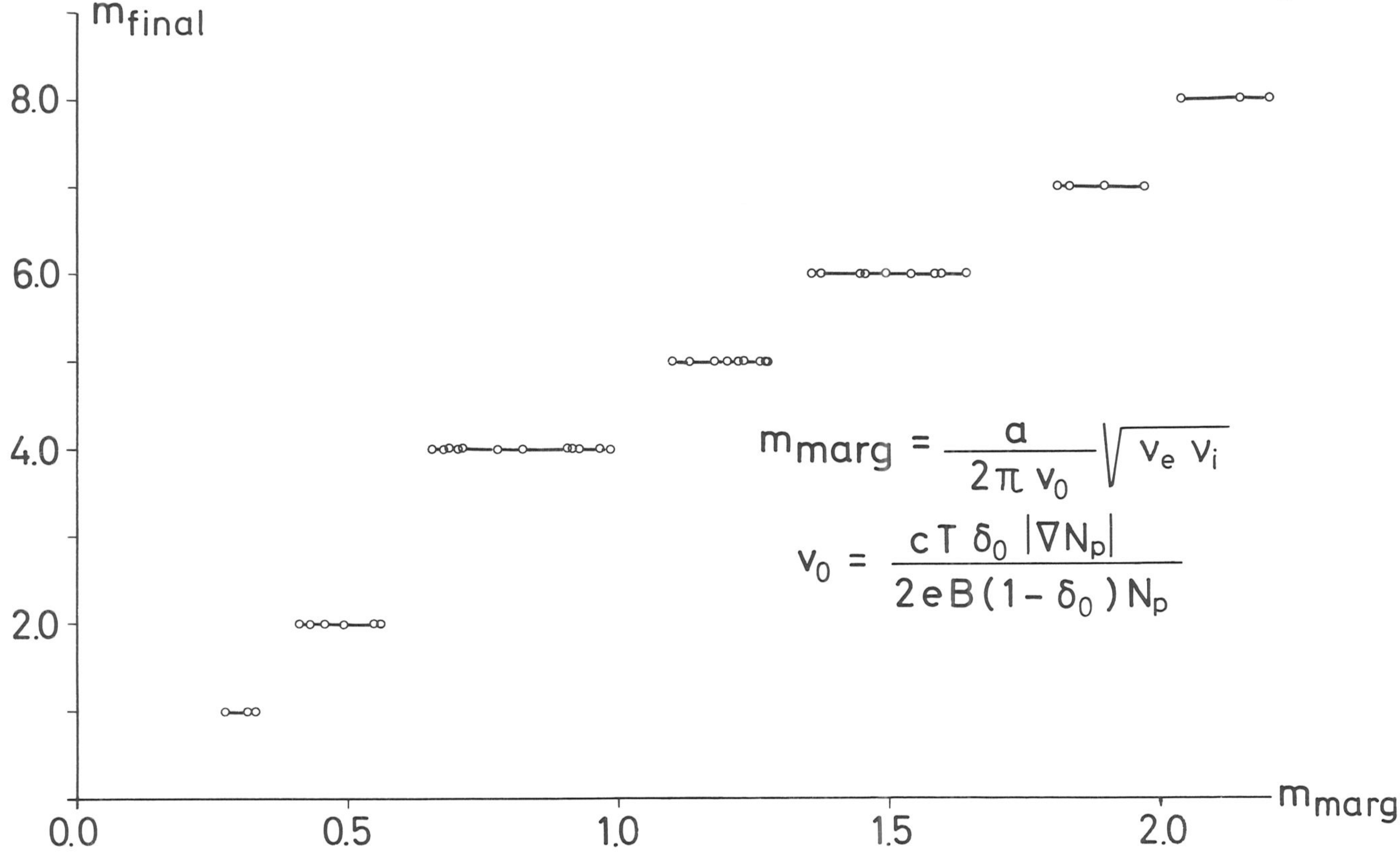

m_{final}
8.0
6.0
4.0
2.0
0.0
0.5
1.0
1.5
2.0
m_{marg}
$m_{marg} = \frac{a}{2\pi v_0}\sqrt{v_e v_i}$
$v_0 = \frac{cT\delta_0 |\nabla N_p|}{2eB(1-\delta_0)N_p}$

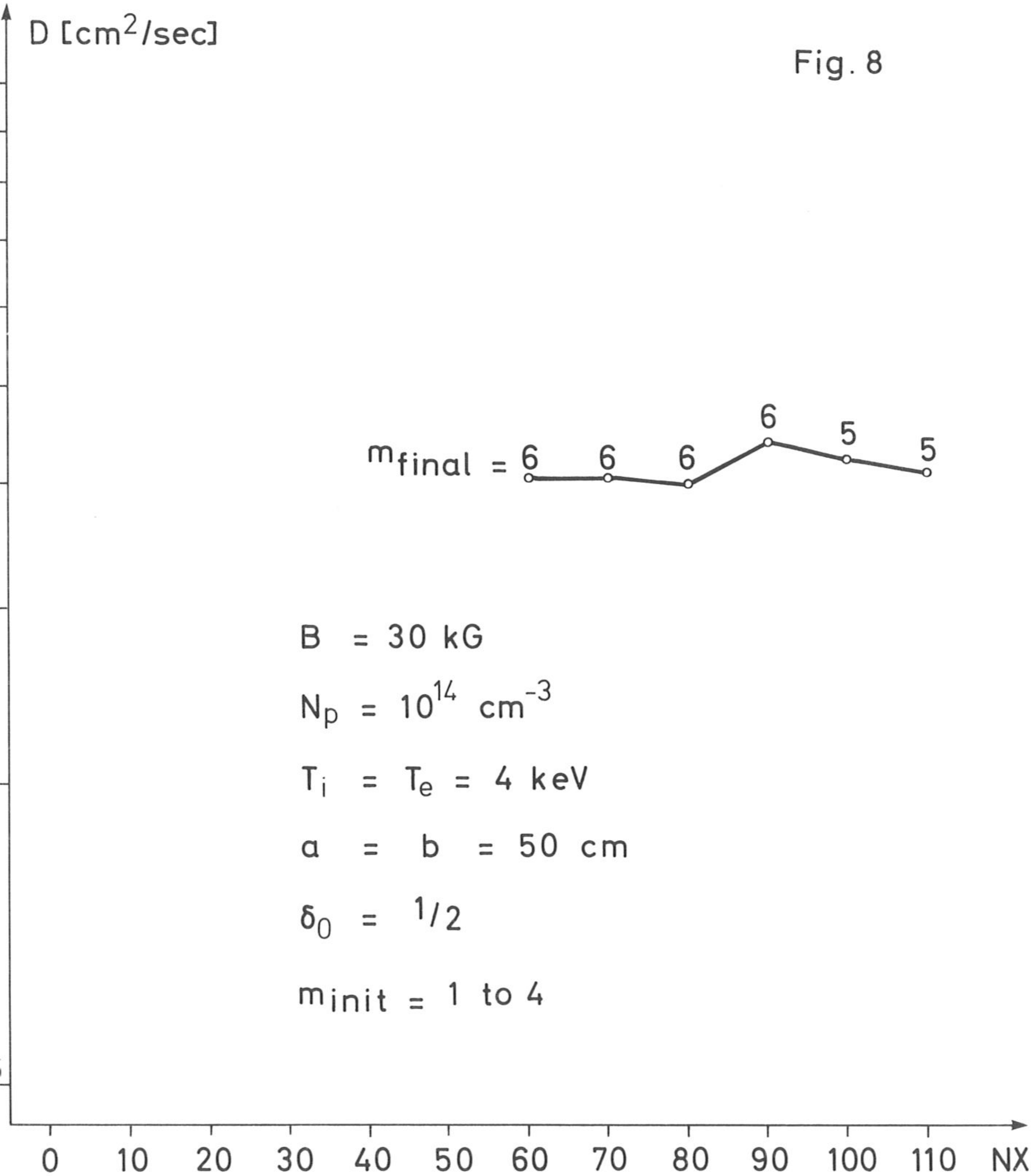
D [cm²/sec]
Fig. 8
m_final = 6 6 6 6 5 5
B = 30 kG
N_p = 10^14 cm^-3
T_i = T_e = 4 keV
a = b = 50 cm
δ_0 = 1/2
m_init = 1 to 4
0 10 20 30 40 50 60 70 80 90 100 110 NX

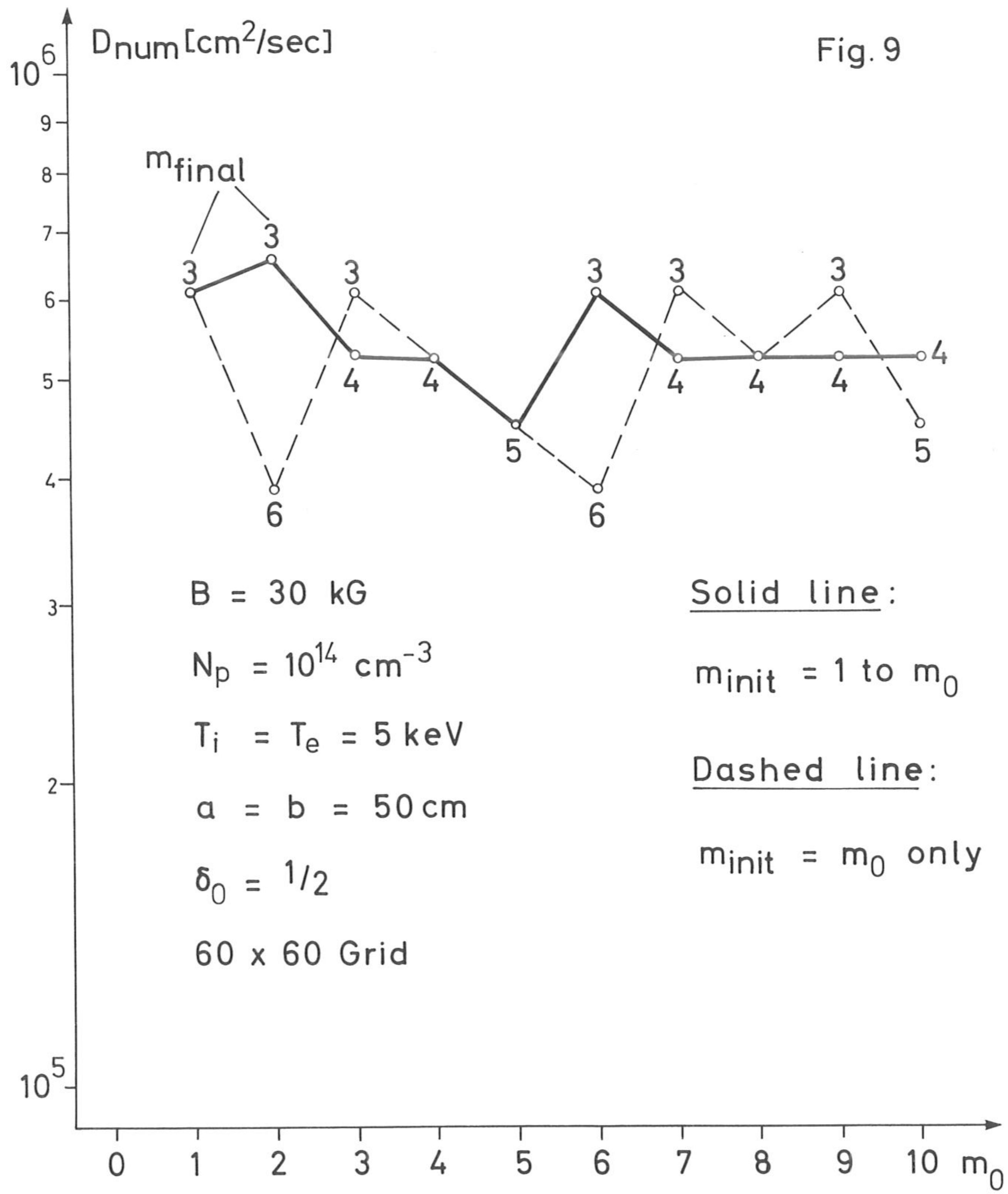
Dnum [cm²/sec]
10⁶
9
8
7
6
5
4
3
2
10⁵
m final
3
3
3
4
4
5
6
3
6
3
4
4
3
4
4
5
B = 30 kG
Np = 10¹⁴ cm⁻³
Ti = Te = 5 keV
a = b = 50 cm
δ0 = 1/2
60 x 60 Grid
Solid line:
minit = 1 to m0
Dashed line:
minit = m0 only
0 1 2 3 4 5 6 7 8 9 10 m0

Fig. 9

Fig. 10

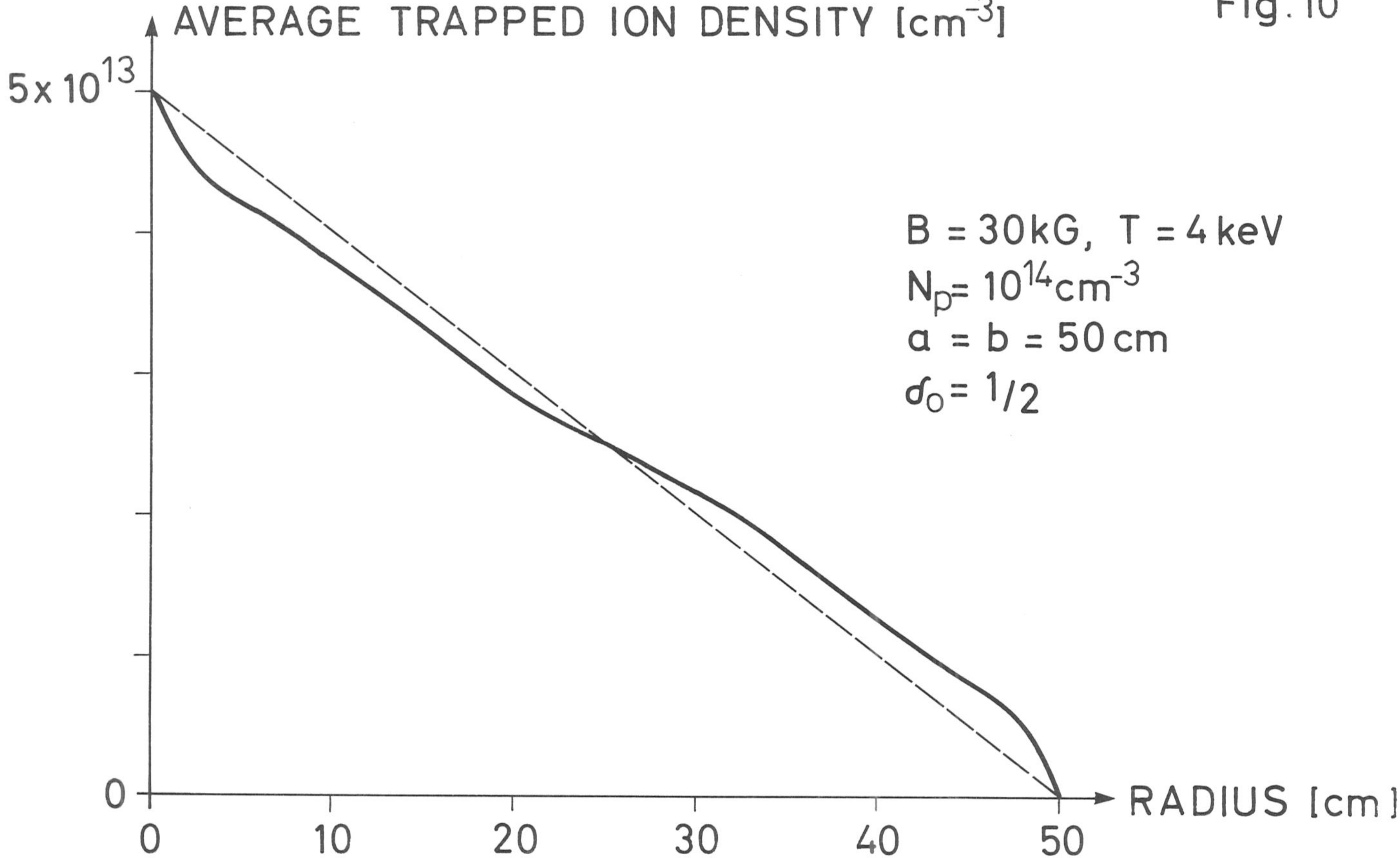
AVERAGE TRAPPED ION DENSITY [cm^{-3}]
5×10^{13}
0
B = 30 kG, T = 4 keV
$N_p = 10^{14}$ cm^{-3}
a = b = 50 cm
$\sigma_0 = 1/2$
0
10
20
30
40
50
RADIUS [cm]